Journal of
Ceramic Science
and Technology

J. Ceram. Sci. Tech., 07 [02] 193-202 (2016)
DOI: 10.4416/JCST2016-00017
available online at: http://www.ceramic-science.com

Mechanical Characterisation of Carbon-Bonded Magnesia at Temperatures up to 1400 °C

J. Solarek*[1], C.G. Aneziris[2], H. Biermann[1]

[1]Institute of Materials Engineering, TU Bergakademie Freiberg, D-09599 Freiberg, Germany
[2]Institute of Ceramic, Glass and Construction Materials, TU Bergakademie Freiberg, D-09599 Freiberg, Germany

received Febuary 12, 2016; received in revised form April 10, 2016; accepted April 15, 2016

Abstract

The mechanical properties of carbon-bonded magnesia were investigated from room temperature to 1400 °C in tension, compression and bending. For this purpose, quasi-static, static and cyclic tests were conducted on two testing machines, equipped with inert atmosphere chambers and inductive heating devices. Characterisation of the microstructure was performed with scanning electron microscopy (SEM) and optical microscopy (OM). Porosity and density were measured with the Archimedes principle and pycnometry. From the creep tests, activation energies and Norton exponents for high-temperature creep deformation were determined. Additionally, scatter was addressed. The cyclic tests showed a high influence of stress amplitude on fatigue lifetime, whereas degradation of specimens only took place in tension.

Keywords: Refractories, high temperature carbon-bonded magnesia, mechanical properties, creep

I. Introduction

Ceramic refractory materials play a key role in manufacturing processes, e.g. steel metallurgy, glass processing or concrete production on account of their stability against chemical decomposition at high temperatures. In particular, carbon-bonded refractories offer excellent thermal shock resistance owing to high thermal conductivity, good plasticity and weak wettability. They are therefore often used when temperature changes cyclically during processing, e.g. in steel ladles or converters. In such applications, carbon-bonded magnesia (MgO-C) has become established as lining material. Nevertheless, wear and erosion caused by the contact with melt and slag limit the lifetime of MgO-C bricks. These loads result in damage of the refractory material and thus high costs for the industry. Therefore, great efforts have been made to investigate the failure behaviour and deliver lifetime predictions over recent decades [1].

However, innovative and complex testing techniques are still required for material characterisation. In particular, it is important to investigate the mechanical behaviour not only at room temperature, but also at high temperatures in quasi-static, static and cyclic tests. Jenkins [2] and Seldin [3] tested several electrode graphite materials, which are relevant for carbon-bonded magnesia since their mechanical properties are influenced mainly by the graphitic matrix. Jenkins [2] tested reactor-grade graphite at room temperature and found micro plasticity and a hysteresis between loading and unloading paths. Seldin [3] investigated the mechanical properties of several graphite grades at room temperature. He found asymmetric behaviour in compression and tension and showed that mechanical loading leads to residual strains, which can be annealed at high temperatures. Fitchett and Wilshire [4] analysed the mechanical behaviour of carbon-bonded magnesia and found a significant influence of heat treatment on mechanical properties at both room temperature and high temperatures. They also stated that carburisation of the material leads to a change in the mechanical behaviour from plastic collapse to brittle failure for pitch- as well as resin-bonded magnesia. Allaire *et al.* [5] investigated the creep behaviour of carbon-bonded magnesia at temperatures of 1100 °C to 1200 °C at low stresses in compression. They found significant amounts of creep at 1000 °C and explained this behaviour based on deformation in the carbonaceous matrix. They concluded that this deformation was caused by the large amount of porosity formed during the heat treatment. Ioka *et al.* [6] introduced acoustic emission to mechanical testing of graphite. They found the dominating mechanism of deformation to change from slip at low stresses to microcracking at high stresses. Investigations of Franklin and Tucker [7] showed an increase of bending strength and stiffness with increasing test temperature up to the coking temperature. This behaviour was explained with closure of cracks and pores which were formed during coking owing to the different thermal expansion of graphite and magnesia. Robin *et al.* [8] and Schmitt *et al.* [9] investigated the mechanical properties of resin- and pitch-bonded magnesia under compression, tension and bending. For the tests, they used an inductive heating device. For coked material, they found values of ultimate tensile strength of about 6.3 to 6.5 MPa and a Poisson ratio of

* Corresponding author: Johannes.Solarek@iwt.tu-freiberg.de

approximately 0.2. The creep behaviour of carbon-containing alumina refractory concrete was analysed by Oerdraogo and Prompt [10,11] who found significant amounts of creep above 800 °C. Analysis of the Young's modulus by Briche *et al.* [12], Kakroudi *et al.* [13] and Werner *et al.* [14;15] revealed that cracks of preheated refractories close during heating with increasing temperature, yielding an increase in the dynamic Young's modulus. Recently, the mechanical properties of carbon-bonded alumina (Al_2O_3-C) and magnesia (MgO-C) were investigated by the authors' group [16–18].

The cyclic behaviour of carbon-bonded refractories was recently investigated from room temperature up to 1400 °C by Hino *et al.* [19], Andreev *et al.* [20] and Ouedraogo and Prompt [10,11]. In compression, fatigue occurred at stresses of 70 % to 80 % of the material strength, whereas degradation of the specimen took place between grains and carbonaceous matrix. For damage behaviour, the maximal compressive stress seemed to play a major role compared to the effective stress amplitude. At higher temperatures, damage behaviour was dominated by creep, not by fatigue processes.

However, the results are difficult to transfer to real application, since tests were conducted in cyclic compression only. Owing to thermal expansion and temperature gradients, stresses are induced in both compression and tension [21] within the magnesia bricks of refractory linings. Additionally, the influence of the combination of thermal and mechanical cycling has not been investigated so far.

The aim of the present work is to investigate the creep as well as cyclic behaviour taking into account both compressive and tensile loading at low and high temperatures, respectively. To gain information about the viscous behaviour, stresses were chosen to be high (2 – 20 MPa) in comparison to standardised tests [22] (up to 0.2 MPa). First results on quasi-static and creep tests have been recently published elsewhere [18,23].

II. Experimental Details

(1) Materials

The tests were performed on three different batches of carbon-bonded magnesia with a maximal MgO grain size of 2 mm, an initial graphite content of 10 % and a binder content of 3.2 % (see Table 1). Batch I was used for static and cyclic tests as well as for stress relaxation tests. Creep tests were performed on batches II and III. The grain size distribution of the magnesia was adjusted using the Dinger-Funk equation [24] with distribution modulus of 0.5 – 0.6. All components were mixed in an Eirich mixer (RV02, Maschinenfabrik Gustav Eirich, Hardheim, Germany) and subsequently pressed. Specimens for bending tests were pressed uniaxially into bars (approx. 145 mm x 25 mm x 25 mm, see Fig. 1a) at a pressure of 150 MPa. For the compression tests, small cylinders were turned out of the bars. For both, bending and compression tests, the pressing direction was parallel to loading axis. After pressing, the materials were heated in stages to 180 °C for polymerisation of the bonding agent and coked under reducing atmosphere at 1000 °C in a coke bed. For batches II and III, half of the specimens were coked at 1400 °C to investigate the influence of the coking temperature on creep behaviour.

Table 1: Components for processing of carbon-bonded magnesia.

Raw material	Product	Manufacturer	wt%
Magnesia	Fused magnesia	Refratechnik Steel GmbH	90.0*
Graphite	Flake graphite NFL 92/94	GraphitKropfmühl GmbH	10.0*
Powder binder	Bakelite® PF 0235 DP	Momentive Speciality Chemicals	1.0
Liquid binder	9950 FL	Momentive Speciality Chemicals	2.2
Bonding additive	Hexamethylenetetramine	INEOS Paraform GmbH & Co KG	0.3

* Graphite and magnesia yield 100 %

Specimens for tensile tests were pressed at 150 MPa in a hydrostatic press, yielding cylindrical billets. These billets were heated in stages to 180 °C for hardening of the binder. Then, cylindrical specimens with a diameter of 30 mm and a height of 80 mm were drilled out of the billets. The cylinders were glued into steel adapters to enable load transfer in tension and compression, using a linear guide to ensure axial specimen alignment. Afterwards, the specimens were coked in a coke bed at 1000 °C in a reducing atmosphere.

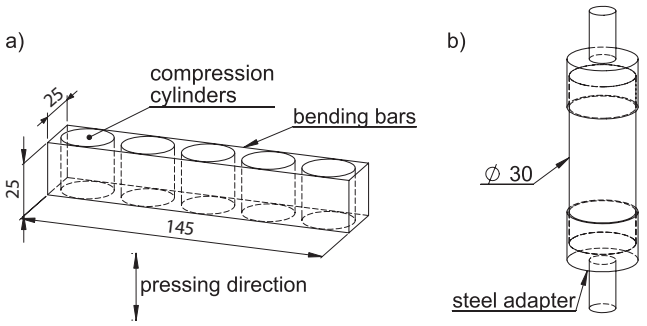

Fig. 1: Specimen geometry for compression and bending tests (a) and tensile and cyclic tests (b).

(2) Experimental methods

The microstructure was characterised with a field emission scanning electron microscope (MIRA 3 XMU, Tescan, Brno, Czech Republic) and optical microscopy (Neophot 30, Carl Zeiss Jena, Jena, Germany). Therefore, specimens were cut, infiltrated with resin, subsequently ground and polished up to a particle size of 1 µm and coated with a thin layer of carbon. For investigation of porosity and density, the Archimedes principle was applied with toluene (C_7H_8) as a medium to prevent hydration of magnesia. The true density was determined with a pycnometer (AccuPyc 1350, Micromeritics, Norcross, USA).

Tests in four-point bending (see Fig. 2a) and compression (see Fig. 2b) were performed using a 20 kN electro-mechanical testing machine (Z020, Zwick, Ulm, Germany) equipped with an inert gas chamber (Maytec, Singen, Germany) and an inductive heating unit (TrueHeat HF 5010, Hüttinger, Freiburg, Germany) with copper coils (2). For testing, the chamber was evacuated and filled with Argon twice. Strain measurement was performed with a high-temperature strain gauge with alumina probes (1). For the compression tests, molybdenum susceptors (TZM, not visible) were placed below and above the specimen to ensure homogeneous temperature distribution. During the tests, the temperature was measured with a pyrometer (MS 09, Sensortherm, Nuremberg, Germany) working at wavelengths of 0.7 µm to 1.1 µm using a thermal emission coefficient of 0.93.

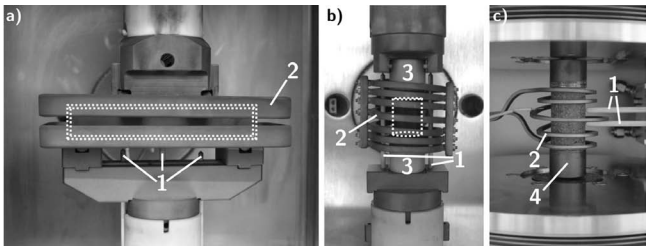

Fig. 2: Test setup for bending tests (a), compression tests (b) and tension and cyclic tests (c): 1 – alumina probes, 2 – copper coils, 3 – Si_3N_4-pistons, 4 – steel adapters. In (a) and (b) samples' contours are outlined with white dashed lines.

Compressive creep tests were carried out for 90 minutes at 10 MPa (batch II) and 20 MPa (batch III). After reaching the test temperature, the system was held constant for 5 minutes to homogenise temperature distribution within the specimens. Stress relaxation tests in compression were carried out for 30 minutes at constant strain with an initial stress of 20 MPa on batch I.

Tensile and cyclic tests were performed using a 100 kN servo-hydraulic universal testing machine (MTS 810, MTS, Berlin, Germany) equipped with a vacuum chamber (Sigmatest, Wedel, Germany), see Fig. 2c. During testing, pressure was below 10^{-1} mbar. Temperature was measured with a pyrometer (PZ 20AF2/D, Keller HCW GmbH, Laggenbeck-Ibbenbüren, Germany) with a working wavelength of 1.1 µm to 1.7 µm. The specimens were heated with an inductive heating device (TrueHeat HF 3005, Hüttinger) and a copper coil (2). Strain was measured using a standard high-temperature extensometer with alumina probes (1). Uniaxial specimen alignment was proven in former tests on a specimen equipped with multiple strain gauges [23]. Heating rates were in the range of 10 to 20 K·sec^{-1} for all tests.

The dynamic Young's modulus E_{dyn} was determined by measurement of sonic propagation time t_{sonic} (BP 7, Steinkamp, Bremen, Germany) through the samples. E_{dyn} was calculated using equation (1), where h is sample height, ϱ is density and µ is Poisson's ratio, which was found in the literature to be approximately 0.2 [8, 9] for MgO-C.

$$E_{dyn} = \left(\frac{h}{t_{sonic}}\right)^2 \cdot \varrho \cdot \frac{(1+\mu)\cdot(1-2\mu)}{1-\mu} \qquad (1)$$

III. Results and Discussion

(1) Microstructure

The microstructure of the material is shown in Fig. 3. The material consists of coarse magnesia grains, embedded in a carbon-rich matrix with fine magnesia particles. Within the coarse magnesia grains, CaO/SiO_2impurities were observed as bright areas (Fig. 3a) with a CaO/SiO_2 mass ratio of 1.5, which was determined with energy-dispersive x-ray spectroscopy (EDX) in SEM. For a wide range of magnesia-based refractories, impurities with CaO/SiO_2 ratios from 1 to 2 are known to form low-temperature melting phases. Nevertheless, the influence of the CaO/SiO_2 mass ratio on the high-temperature behaviour of carbon-bonded magnesia is not conclusively described in the literature. Whereas generally a decrease of mechanical strength is related to such impurities, only minor influences were reported by Allaire *et al.* [5].

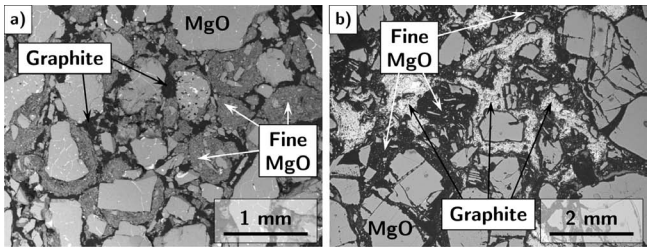

Fig. 3: Microstructure of MgO-C in SEM back-scattered electron contrast (a) and with an optical microscope (b).

The microstructure reveals several cracks within the magnesia grains, which were formed during pressing at 150 MPa. Moreover, cracks within the matrix and between matrix and magnesia grains were observed. These cracks result from different thermal expansion coefficients of magnesia and graphite and are generated during cooling from the heat treatment (i.e. coking temperature) as stated in literature [7, 12–15].

(2) Quasi static tests

The mechanical behaviour of carbon-bonded magnesia was tested at room temperature in quasi static tests under bending, compression and tension. The results are presented in Table 2. A representative stress-strain curve for compressive loading is shown in Fig. 4a. The black line shows the course of a compression test which was stopped at 16 MPa. At the beginning of the tests, a pronounced running in characteristic can be seen owing to deformation of the bases of the cylinders. After unloading, small amounts of plastic deformation remained. Additionally, a pronounced hysteresis between loading and unloading path was observed. On further loading, the hysteresis width was closed nearly completely (dashed grey line). This reveals that the material showed small amounts of inelasticity and microplasticity even at room temperature. When tested until fracture, the slope of the course decreases owing to growth and unification of cracks (solid grey line). At ultimate compression strength, brittle failure occurs. This behaviour is in good agreement with observations from graphite- [2, 3] and carbon-bonded refractories [8].

Table 2: Mechanical properties of carbon-bonded magnesia (batch I, T_{coke} = 1000 °C) at RT.

	Bending	Compression	Tension
Number of tests	21	8	7
Ultimate strength	2.4 ± 0.2 MPa	26.5 ± 0.5 MPa	0.69 ± 0.11 MPa
Elongation at fracture	0.12 ±0.02 mm	-	0.11 ±0.08 %
Young's modulus	-	2.3/10.1 GPa*	2.8 ±1.3 GPa

* Young's modulus from loading/unloading path

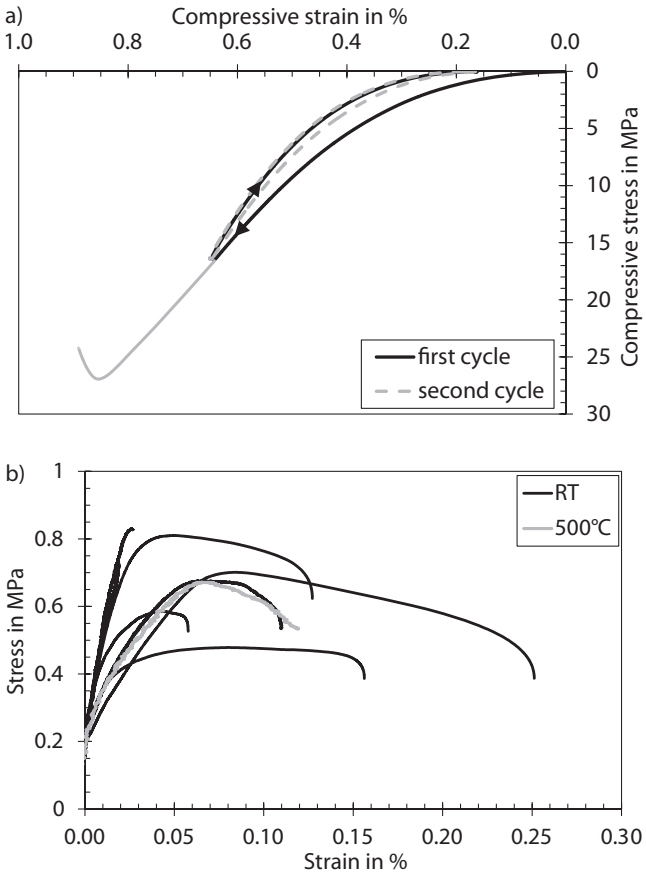

Fig. 4: Stress-strain curves of MgO-C at RT at first loading/unloading (black solid line), at second loading/unloading (grey dotted line) and up to fracture (grey solid line) in compression (a) and in tension (b) at RT (black lines) and 500 °C (grey line).

In tension tests on seven specimens, a short linear stage in terms of Hooke's law with a slope of 2.8 ±1.3 GPa was observed above a preliminary test force of 0.2 MPa. Again, the curves revealed small amounts of microplasticity. Nevertheless, no visible macroscopic plastic deformation was found on the fracture surfaces. The specimens revealed strength of approx. 0.69 ± 0.11 MPa. This is relatively low compared to tensile strength reported by Robin *et al.* [8] and Schmitt *et al.* [9] for carbon-bonded magnesia coked at 500 °C. These authors found values between 6.25 and 6.5 MPa in so-called PIED tests, where ceramic specimens were glued onto steel plates. With this method, unstable crack growth is prevented, leading to higher tensile strengths. In addition, the strength of carbon-bonded refractories decreases with increasing coking temperature [7]. Nevertheless, the courses of the curves were comparable to those reported in the present work.

No change in behaviour was found in a test at 500 °C, since no thermally activated mechanisms occur at this temperature. The mechanisms of deformation do not change between room temperature and 500 °C in quasi-static tests. This matches reports from Ouedraogo and Prompt [10,11] who found no change in behaviour between RT and 400 °C in indirect tension tests.

(3) Dynamic Young's modulus

To investigate the dynamic Young's modulus, analysis of the longitudinal sonic velocity was carried out on five specimens of MgO-C coked at 1000 °C and 1400 °C, respectively. The measurements led to sonic velocities of 1300 m/s (T_{coke} = 1000 °C) and 1180 m/s (T_{coke} = 1400 °C). Eq. 1 with a Poisson ratio of 0.2 [8,9] and the density 3.39 g·mm^{-3} gives a dynamic Young's modulus of 3.6 ± 0.1 GPa (T_{coke} = 1000 °C) and 3.5 ± 0.1 GPa (T_{coke} = 1400 °C). These results are high in comparison with the results from the quasi-static tests. In general, dynamic methods for determination of the elastic constants deliver higher values [9,12].

(4) Creep tests

For investigation of the mechanisms of deformation at high temperatures, creep tests were carried out at different temperatures from 900 °C to 1400 °C on MgO-C coked at 1000 °C and 1400 °C, respectively. To investigate the influence of load, stresses were varied between batch II (10 MPa) and batch III (20 MPa). Fig. 5 shows a typical course of strain (black line) and strain rate (grey line) as a function of time with two pronounced stages. At the beginning of the test, primary creep occurs. The strain rate decreases with ongoing time. After some time, the creep curve shows a point of inflection with a minimal creep rate. Afterwards, the creep rate increases continuously until fracture takes place at the end of the test. There was no evidence of stationary creep with a constant minimal creep rate.

The influence of temperature on creep behaviour was investigated at different stresses (10 MPa and 20 MPa) and different coking temperatures (1000 °C and 1400 °C). Fig. 6 shows the evolution of the creep curves (a) and the differentiated creep curves (b) for different temperatures. Whereas nearly no creep occurred until 1100 °C, the creep rate increased rapidly above this temperature. This increase of creep rate above 1000 °C to 1100 °C was found for all materials, no matter whether they had been coked at 1000 °C or 1400 °C. At 1300 °C, resistance of the material against static deformation decreased significantly, leading to failure within 15 minutes. These observations are in reasonable agreement with results from Ouedraogo and Prompt [10,11], who found brittle to ductile transition between 900 °C and 1000 °C. They found creep deformation at and above 800 °C. For fine-grained carbon-bonded alumina, a threshold temperature of approx. 1050 °C was found by the authors [17].

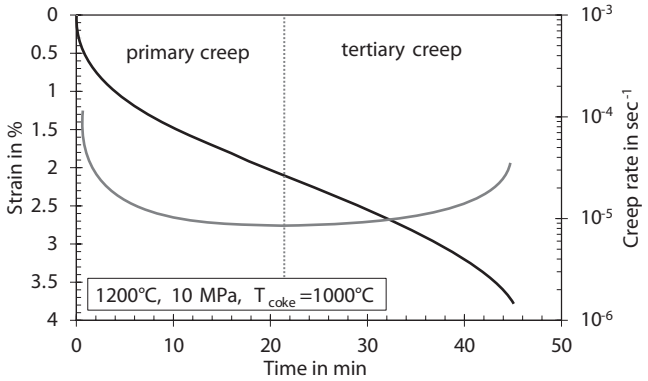

Fig. 5: Results of creep test of MgO-C (T_{coke} = 1000 °C) at a compressive stress of 10 MPa (batch II) at 1200 °C: Creep strain and creep rate vs. time.

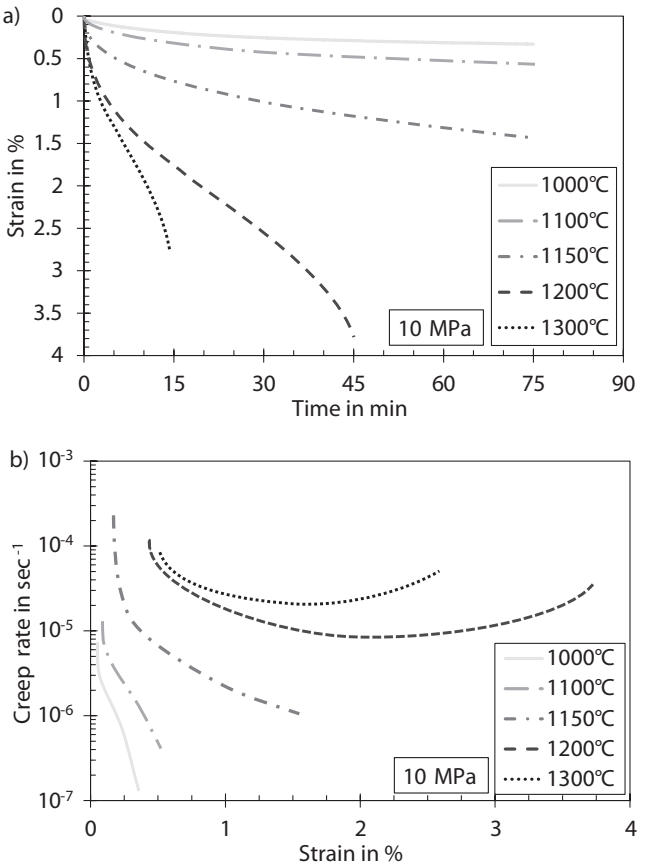

Fig. 6: Creep curves (a) and differentiated creep curves (b) of MgO-C coked at 1000 °C at different temperatures at a compressive stress of 10 MPa (batch II).

With increasing temperature, elongation at fracture decreased when tertiary creep was reached. This was due to increased creep rates with premature onset of tertiary creep deformation, as visible in Fig. 6b. This behaviour was found for all batches.

Not all specimens reached tertiary creep within the test duration of 90 minutes. Below 1100 °C no tertiary creep was observed at all. All specimens tested above 1200 °C showed tertiary creep. At temperatures from 1100 °C to 1200 °C, tertiary creep was obtained for some specimens.

From the dependence of the minimal creep rate on temperature, activation energies were determined at 10 MPa (batch II) and 20 MPa (batch III) for materials coked at 1000 °C and 1400 °C. Only specimens that reached tertiary creep with a pronounced point of inflection within the creep curve were used for this evaluation. For determination of the activation energy Q_C, the following equation was used:

$$Q_C = -2.304 \cdot R \cdot \frac{d(\lg \dot{\varepsilon}_{min})}{d(1/T)} \qquad (2)$$

where R is the gas constant, $\dot{\varepsilon}$ is the minimal creep rate and T is the test temperature. The results are given in Fig. 7a for different batches (with different stresses) and coking temperatures. There is no distinct influence of the coking temperature on the minimal creep rate. A change in mechanisms can be seen in the results of batch III (T_{coke} = 1400 °C). Below 1200 °C, creep rate increases only moderately as temperature rises with an activation energy of only Q_C = 163 kJ/mol. This is in good agreement with observations of Allaire *et al.* [5], who found an activation energy of Q_C = 188 kJ/mol for carbon-bonded magnesia with 10 % graphite between 1100 MPa and 1200 °C. Above 1200 °C, the minimal creep rate increases rapidly with increasing temperature, leading to an activation energy of Q_C = 935 kJ/mol. This phenomenon with a sharp increase of the creep rate above a threshold temperature of approximately 1200 °C was observed for other test series (batch II – T_{coke} = 1400 °C, batch III – T_{coke} = 1000 °C) as well, see Fig. 6a for example. However, these data were not considered since no tertiary stage was reached.

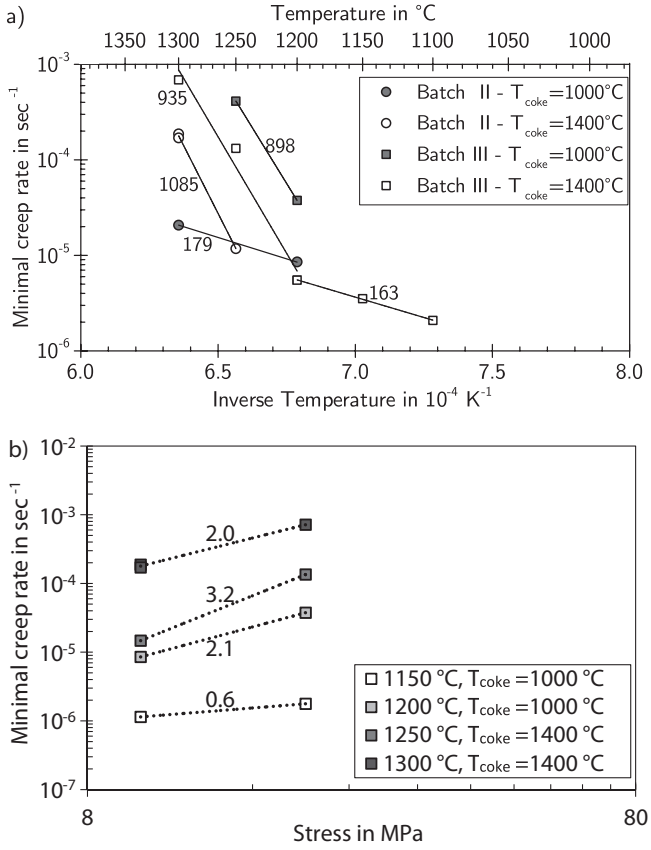

Fig. 7: Minimal creep rates of MgO-C as a function of inverse temperature (a) and stress (b) for different coking temperatures. The diagrams include trend lines with estimated activation energies Q_C (kJ/mol, a) and Norton exponents n (b). Each dot represents the minimal creep rate of one experiment.

The activation energies of these test series were in the range of 889 to 1085 kJ/mol at high temperatures, which is high compared to activation energies recorded for creep in general. Terzic *et al.* [25] reported activation energy of 344 kJ/mol for tar-bonded magnesia between 1350 °C and 1510 °C. It was not possible to connect a microstructural mechanism with such high activation energies. Nevertheless, a much lower activation energy of 179 kJ/mol was registered in one test series (batch II – T_{coke} = 1000 °C) between 1200 °C and 1300 °C. The reasons for these large differences are not known yet.

Generally, tests at 10 MPa deliver lower minimal creep rates compared to tests carried out at 20 MPa. To determine the Norton exponent *n*, the data were analysed using equation 3. Again, only tests which showed tertiary creep were included. The results are shown in Fig. 7b, where the minimal creep rates are plotted as a function of stress for different temperatures. At temperatures above 1150 °C, *n* equals values from 2.0 to 3.2. This matches well with Norton exponents from fine-grained carbon-bonded alumina [17] ($n = 2.3$) and carbon-bonded magnesia/dolomite [5] ($n = 2-3$) reported in literature. At 1150 °C, *n* was found to be 0.6, indicating only small influence of stress. Nevertheless, it has not yet been established whether scatter or an actual change in creep mechanisms led to this small Norton exponent.

$$\dot{\varepsilon}_{min} \sim \sigma^{n} \tag{3}$$

(5) Ex-situ microstructural investigation

The microstructure after high-temperature deformation was investigated with optical light microscopy and SEM. In most cases, no significant changes in the microstructure were observed. Only in specimens tested at high temperatures, which reached a late stage of tertiary creep, intense crack networks were observed. Such a microstructure is shown in Fig. 8 on a specimen tested at 1300 °C and a stress of 10 MPa (batch II) with the corresponding creep curve. The specimen shows numerous cracks through its cross-section. Most cracks were found at the edges of the specimen whereas fewer cracks were found on the faces of the cylinder. The cracks are orientated parallel to stress direction and mainly appear within the matrix and between magnesia and the carbonaceous matrix, as visible in the detailed view in Fig. 8b. Cracked particles of magnesia were observed along the crack paths only in some cases. There was no evidence for deformation of magnesia particles owing to formation of low-temperature melting phases of silica and calcium oxide. This matches with the observations of Allaire *et al.* [5], who found only a minor influence of CaO/SiO_2-impurities with mass ratios of 1 – 2 on the creep of carbon-bonded magnesia.

(6) Scatter of the creep tests

To estimate the range in which creep curves scatter within one set of parameters, five tests were performed at a temperature of 1200 °C and a stress of 10 MPa on specimens of one batch coked at 1400 °C. The results are shown in Fig. 9 as creep strain (a) and creep rate (b) as a function of time with black lines. The curves show some scatter. The creep rate at the end of the tests after 90 minutes differs only by a factor of two between $8.5 \cdot 10^{-7}$ sec^{-1} and $2.0 \cdot 10^{-6}$ sec^{-1}. This range is small compared to the differences caused by changes of temperature to 1100 °C or 1250 °C (grey lines). Anyway, the minimal creep rate is not only influenced by the thermodynamic behaviour of the material at high temperatures, but also by the biggest defect or crack within the specimen. Therefore, scatter still needs to be addressed with a larger number of specimens in future work.

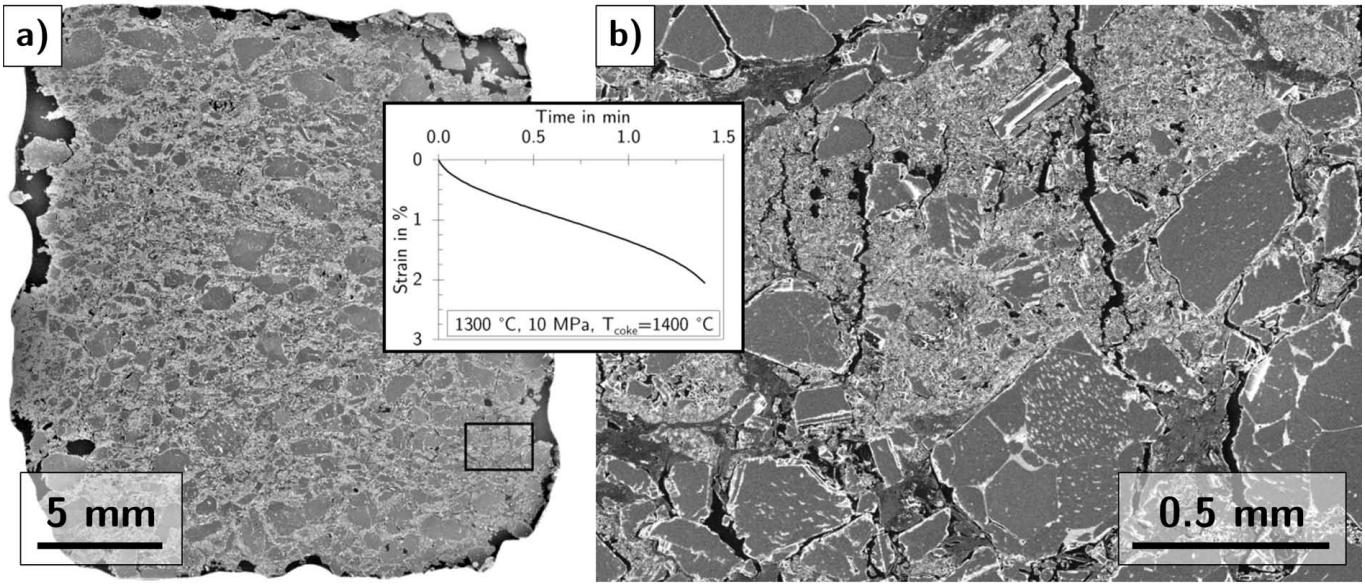

Fig. 8: Cross-section of MgO-C after a creep test at 1300 °C under compressive load of 10 MPa (batch II, T_{coke} = 1400 °C). a) Overview, b) details at higher magnification. The corresponding creep curve is shown in the insert. Stress axis vertical.

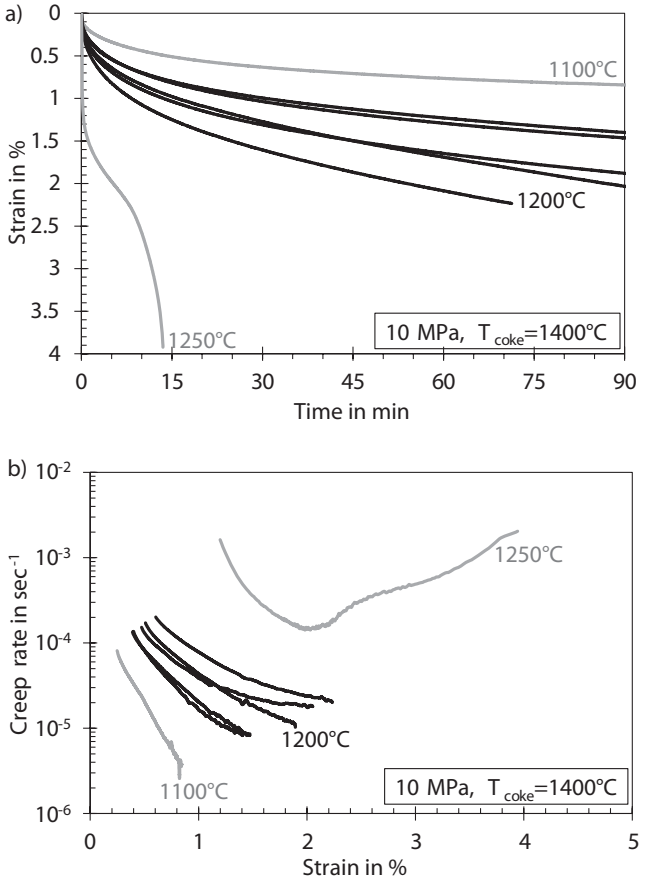

Fig. 9: Creep curves (a) and differentiated creep curves (b) of MgO-C under a compressive stress of 10 MPa (batch II, T_{coke} = 1400 °C) at 1200 °C (grey lines: 1100 °C and 1250 °C).

(7) Stress relaxation tests

In addition to the creep tests, mechanical behaviour was investigated by means of stress relaxation tests at RT and between 700 °C and 1300 °C. At room temperature, stress relaxation led to a decrease in stress of approx. 8.0 % from 20 MPa to 18.4 MPa, which is in good agreement with results of Robin *et al.* [8] who found a relaxation of 15 % for uncoked resin-bonded magnesia. This matches observations from quasi-static tests, where microplasticity was found in the form of pronounced hysteresis within the first loading cycles, see Fig. 4a.

At temperatures of and above 700 °C, stresses of 20 MPa were released nearly completely within 30 minutes to less than 2 MPa, see Fig. 10a. Even at moderate temperatures of 700 °C the ability to release stresses through plastic deformation is highly developed. In Fig. 10b, remaining stresses after certain times are plotted versus test temperature. With increasing temperature, stress was released more quickly.

This behaviour is important for typical applications of carbon-bonded magnesia, such as for steel ladles and converters. Thermal stresses caused during heating are reduced quickly, leading to small stresses at both moderate and high temperatures. Nevertheless, the occurring mechanisms are not inexhaustible, which was shown for carbon-bonded alumina [17]. This means, development of thermal stress within the lining will change with ongoing time of operation. The observed behaviour has to be addressed in numerical simulations of stress development in converters or steel ladles and can be used to explain the huge differences between simulations [26,27] (up to and above 100 MPa) and strength of the material. Moreover, it leads to the suggestion of low heating rates in refractory linings. Low heating rates yield not only small temperature gradients and therefore low thermal strains, they also allow relaxation of stress within the material.

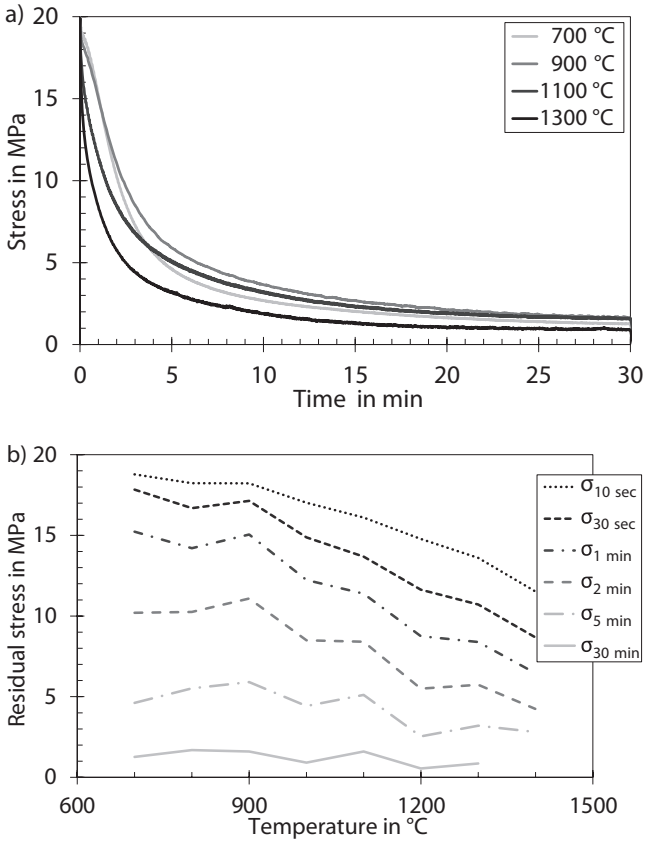

Fig. 10: Evolution of stress as a function of time from stress relaxation tests of MgO-C (batch I, T_{coke} = 1000 °C) at different temperatures (a) and residual stress after certain times as a function of test temperature (b).

(8) Ex situ Young's modulus and porosity

For some specimens, the dynamic Young's modulus and porosity were determined after the tests. The results are presented in Fig. 11 as a function of the test temperature. In the case of the dynamic Young's modulus, no influence was found until approx. 1100 °C. Above 1100 °C, the dynamic Young's modulus increases significantly. This increase in stiffness was observed even when specimens had reached the tertiary stage and showed major cracks through the whole specimen and was thought to be based on specimen densification. However, investigations of total porosity did not support this assumption. The initial total porosity of 14.6 % (T_{coke} = 1000 °C) increased when tests were performed above an threshold temperature of approximately 1000 °C to 1200 °C, see Fig. 11b. This observation can be explained by cracks formed during testing. These cracks led to increased porosities when measured with the Archimedes principle.

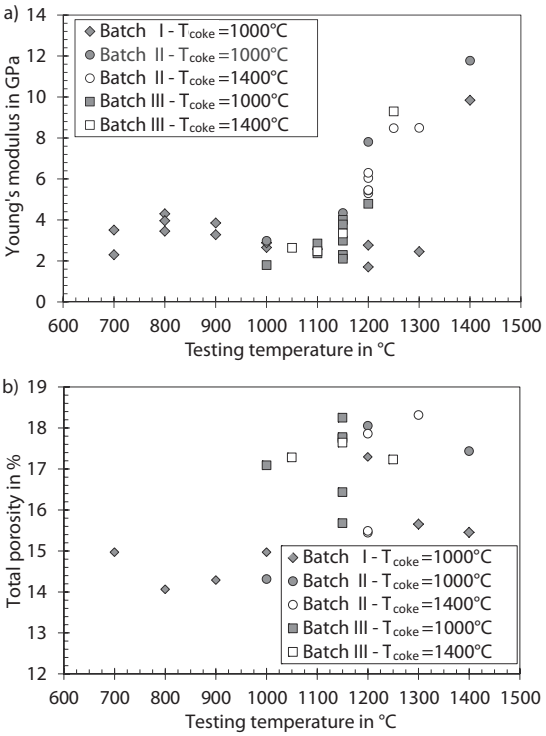

Fig. 11: Dynamic Young's modulus (a) and total porosity (b) as a function of test temperature for stress relaxation tests (batch I) and creep tests (batches II and III), determined *ex situ*.

(9) Cyclic tests

For investigations of the material behaviour under cyclic load, tests were carried out in symmetrical tension/compression ($R = \sigma_{min}/\sigma_{max} = -1$) at a stress amplitude of 0.3 MPa at room temperature for 20 000 cycles. As already observed in room temperature compression tests, a stress-strain hysteresis between loading and unloading path was found, see grey line in Fig. 12a. Nevertheless, a closure of the hysteresis, as observed in repeated compression tests, was not observed in these cyclic tests. This can be attributed to microcracking being closed during compression, but then opened again under tensile loading. Within the first cycle, microcracking occurred, leading to small amounts of irreversible plastic strain. This mechanism continued in the following cycles, leading to a shift of the hysteresis loops towards tensile strains and to a softening of the specimen within the first 5 000 cycles, as visible in the cyclic deformation curve (Fig. 12b) as an increase in strain amplitude. After that, cyclic stability was observed until the test was stopped at 20 000 cycles.

The specimen tested at a stress amplitude of 0.3 MPa was subsequently tested at stress amplitude of 0.35 MPa. A softening of the specimen was observed after the first cycles, leading to failure of the specimen at 187 cycles, see Fig. 13b. As visible in the hysteresis loop (Fig. 13a), degradation of the specimen only takes place in tension but not in compression. The specimen behaviour was completely stationary at $\sigma_a = 0.3$ MPa after 20 000 cycles, but failed within 187 cycles at $\sigma_a = 0.35$ MPa. Thus, cyclic behaviour shows a high influence of stress amplitude on lifetime. At 0.30 MPa, no plastic deformation or growth of cracks occurred. At 0.35 MPa, microcracks combine, leading to an increase in strain amplitude. This degradation only takes place in tension when tested in symmetrical tension/compression tests. Once a crack is formed, unstable crack growth takes place, leading to failure of the specimen within the last cycle, whereas no macroscopic deformation was found on the crack surfaces.

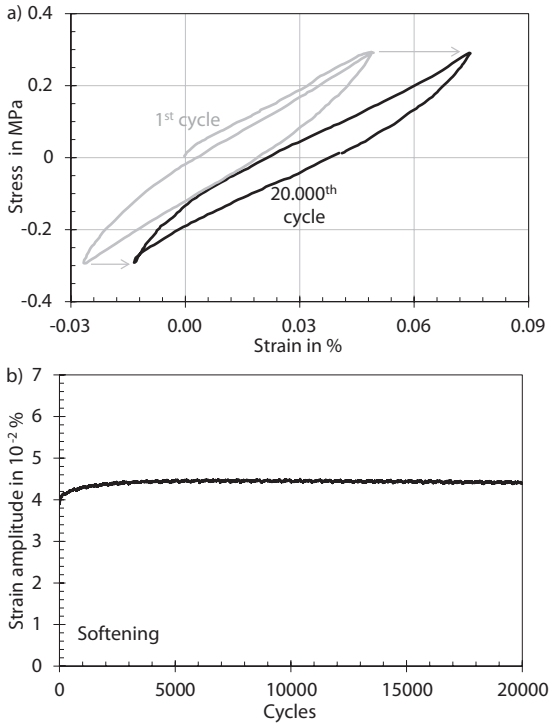

Fig. 12: Stress-strain hysteresis loop of first cycle and after 20 000 cycles (a) and cyclic deformation curve (b) of MgO-C (batch I, T_{coke} = 1000 °C) at room temperature and a stress amplitude of 0.3 MPa.

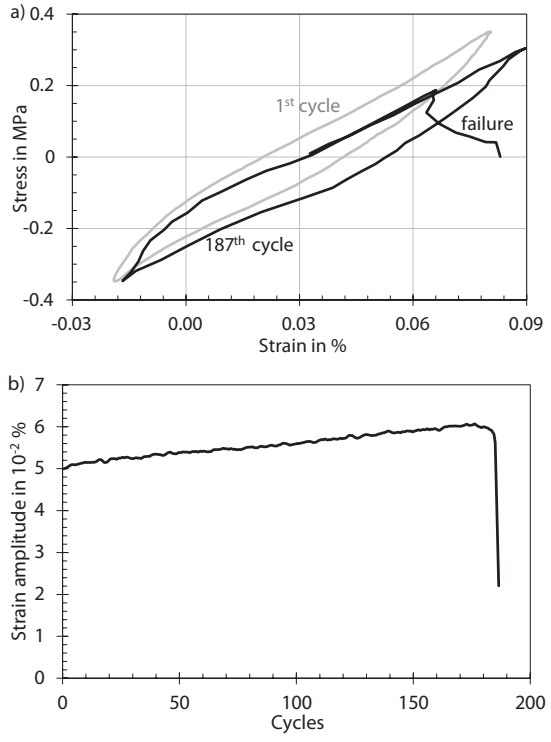

Fig. 13: Stress-strain hysteresis loop of first and last cycle (a) and cyclic deformation curve (b) of MgO-C (batch I, T_{coke} = 1000 °C) at room temperature with a stress amplitude of 0.35 MPa. The specimen was pre-deformed at a stress amplitude of 0.3 MPa for 20 000 cycles.

IV. Summary and Conclusions

Carbon-bonded magnesia shows complex behaviour at both low and high temperatures on mechanical testing. At room temperature a pronounced hysteresis was found between first loading and unloading. This means that even at room temperature without thermal activation small amounts of plasticity occur. Comparable observations were made on graphite [3], which indicates that mechanical behaviour is dominated by the carbonaceous matrix. Nevertheless, failure always occurred owing to brittle failure with unstable crack growth in compression, bending and tension. This behaviour did not change until 500 °C.

Additionally, stress relaxation tests showed minimal visco-plastic deformation at room temperature since stress was reduced by 8.0 % within 30 minutes. Further aspects of the time-dependent deformation behaviour are the differences in Young's modulus for static (2.3 to 2.8 GPa) and dynamic (3.5 to 3.6 GPa) methods. Dynamic values are higher since higher strain rates of the dynamic measurements lead to enhanced mechanical strength and stiffness.

At high temperatures, visco-plastic behaviour dominates the behaviour at static loading. Above 1000 °C, creep increases significantly, leading to fast failure at temperatures of and above 1200 °C at a compressive stress of 10 MPa to 20 MPa within 90 minutes. Nevertheless, stress relaxation tests showed that even at 700 °C the material is able to release stresses of 20 MPa almost completely within 30 minutes by means of plastic deformation. The high-temperature deformation behaviour changes at approx. 1200 °C. Whereas a low activation energy of 163 kJ/mol was found below 1200 °C, high energies of 898 to 1085 kJ/mol were observed above. Nevertheless, one batch showed small activation energies even above 1200 °C. Evaluation of the influence of stress on minimal creep rate led to Norton exponents between 2.1 and 3.1 at 1200 °C to 1300 °C.

SEM observations of specimens tested in creep revealed crack growth between magnesia grains and matrix and within the matrix as the dominating mechanism of deformation and damage. Nevertheless, since specimens showed final creep strains up to 4 %, additional mechanisms like slip along graphitic basal planes seem to appear within the carbonaceous matrix. As a whole, these mechanisms lead to an increase in Young's modulus and porosity when the specimens were tested at and above 1200 °C.

The influence of scatter on the test results was ambivalent. Five identical tests revealed only small scatter of the results. Nevertheless, repetition of whole test series with only slightly changed parameters led to high differences, for example in activation energy, Norton exponent and minimal creep rate. Therefore, the scatter of results still has to be addressed with large amounts of specimens.

Cyclic tension/compression tests at room temperature showed a high influence of stress on fatigue lifetime. Whereas no failure occurred at $\sigma_a = 0.3$ MPa within 20 000 cycles, the same specimen failed quickly at $\sigma_a = 0.35$ MPa after 187 cycles only. Damage occurred exclusively in tension, leading to brittle failure.

Within the cyclic tests, no evidence for a difference in the elastic constants between compression and tension was found. At the transition from compression to tension and vice versa, no change in sample stiffness and no sudden discontinuity were observed. This matches observations from quasi-static tension and compression tests, where comparable Young's moduli (2.3 GPa to 2.8 GPa) were measured.

Acknowledgement

The authors gratefully acknowledge the German Research Foundation (DFG) for financial support of the project under grant number BI 418/28 – 1 within Priority Programme 1418 "FIRE". In addition, the authors would like to thank Refratechnik Steel GmbH (Düsseldorf) for providing the magnesia and Ms Petra Kästner (Institute of Mechanics and Fluid Dynamic) for sample preparation. Furthermore, thanks are due to the Institute of Ceramic, Glass and Construction Materials, where the materials were prepared.

References

1 Ewais, E.M.M.: Carbon based refractories, *J. Ceram. Soc. Jpn.*, **112**, 517 – 532, (2004).

2 Jenkins, G.M: Analysis of the stress-strain relationships in reactor grade graphite, *Br. J. Appl. Phys.*, **13**, 30 – 32, (1962).

3 Seldin, E.J.: Stress-strain of polycrystalline graphites in tension and compression at room temperature, *Carbon*, **4**, 177 – 191, (1966).

4 Fitchett, A.M., Wilshire, B.: Mechanical properties of carbon-bearing magnesia: parts I, II and III, *Trans. J. Br. Ceram. Soc.*, **83**, 54 – 76, (1984).

5 Allaire, C., Daillaire, S., Rigaud, M.: Creep behaviour of natural dolomite carbon-bonded magnesite bricks, *J. Can. Ceram. Soc.*, **56**, 45 – 48, (1987).

6 Ioka, I., Yoda, S., Konishi, T.: Acoustic emission for polycrystalline graphite under compressive loading, *Carbon*, **28**, 489 – 495, (1990).

7 Franklin, S.A., Tucker, B.J.S.: Hot strength and thermal-shock resistance of magnesia-carbon refractories, *Br. Ceram. Trans.*, **94**, 151 – 156, (1995).

8 Robin, J.M., Berthaud, Y., Schmitt, N., Poirier, J., Themines, D.: Thermomechanical behaviour of magnesia-carbon refractories, *Br. Ceram. Trans.*, **97**, 1 – 11, (1998).

9 Schmitt, N., Berthaud, Y., Poirier, J.: Tensile behaviour of magnesia carbon refractories, *J. Eur. Ceram. Soc.*, **20**, 2239 – 2248, (2000).

10 Ouedraogo, E., Prompt, N.: High-temperature mechanical characterisation of an alumina refractory concrete for blast furnace main trough. *J. Eur. Ceram. Soc.*, **28**, 2867 – 2875, (2008).

11 Prompt, N., Ouedraogo, E.: High temperature mechanical characterisation of an alumina refractory concrete for blast furnace main trough, *J. Eur. Ceram. Soc.*, **28**, 2859 – 2865, (2008).

12 Briche, G., Tessier-Doyen, N., Huger, M., Chotard, T.: Investigation of the damage behaviour of refractory model materials at high temperature by combined pulse echography and acoustic emission techniques, *J. Eur. Ceram. Soc.*, **28**, 2835 – 2843, (2008).

13 Kakroudi, M.G., Yeugo-Fogaing, E., Huger, M., Gault, C., Chotard, T.: Influence of the thermal history on the mechanical properties of two alumina based castables, *J. Eur. Ceram. Soc.*, **29**, 3197 – 3204, (2009).

14 Werner, J., Aneziris, C.G., Dudczig, S.: Young's modulus of elasticity of carbon-bonded alumina materials up to 1450 °C, *J. Am. Ceram. Soc.*, **96**, 2958 – 2965, (2013).

15 Werner, J., Aneziris, C.G., Schafföner, S.: Influence of porosity on Young's modulus of carbon-bonded alumina from room

temperature up to 1450 °C, *Ceram. Int.*, **40**, 14439 – 14445, (2014).

16 Solarek, J., Bachmann, C., Klemm, Y., Aneziris, C.G., Biermann, H.: Mechanical Characterisation of Carbon Bonded Alumina (Al_2O_3-C) at temperatures up to 1500 °C. In: Proceedings of the Unified International Technical Conference of Refractories. Vienna, Austria, September 15.-18. 2015

17 Solarek, J., Bachmann, C., Klemm, Y., Aneziris, C.G., Biermann, H.: High-temperature compression deformation behaviour of fine-grained carbon-bonded alumina, *J. Am. Ceram. Soc.*, in press, (2016)

18 Solarek, J., Adlmaier, F.X., Aneziris, C.G., Biermann, H.: High Temperature Behaviour of Carbon Bonded Magnesia (MgO-C) at Temperatures up to 1500 °C. In: Proceedings of the Unified International Technical Conference of Refractories. Vienna, Austria, September 15.-18. 2015

19 Hino, Y., Yoshida, K., Kiyota, Y., Kuwayama, M.: Fracture mechanics investigation of MgO-C bricks for steelmaking by bending and fatigue failure tests along with x-ray CT scan observation, *ISIJ Int.*, **53**, 1392 – 1400, (2013).

20 Andreev, K., Boursin, M., Laurent, A., Zinngrebe, E., Put, P., Sinnema, S.: Compressive fatigue behaviour of refractories with carbonaceous binders, *J. Eur. Ceram. Soc.*, **34**, 523 – 531, (2014).

21 Hampel, M.: Contribution for the Characterization of Carbon Bonded Magnesia Refractories, in German, Dissertation at TU Bergakademie Freiberg, (2011).

22 Norm DIN EN 993: Methods of testing dense shaped refractory products – Part 8 and 9, (1997)

23 Solarek, J., Aneziris, C.G., Biermann, H.: Mechanical properties of carbon-bonded magnesia between room temperature and 1300 °C, in German, in DKG-Handbuch Technische Keramische Werkstoffe - Chap. 6.2.3.2, HvB Verlag, Ellerau, 2015

24 Funk, J.E., Dinger, D.R.: Derivation of the Dinger-Funk Particle Size Distribution Equation. In: Predictive Process Control of Crowded Particulate Suspensions, Springer US, Boston, MA, 1994.

25 Terzic, A., Pavlovic, Lj., Milutinovic-Nikolic, A.: Influence of the phase composition of refractory materials on creep, *Sci. Sinter.*, **38**, 255 – 263, (2006).

26 Rathner, R., Knauder, J.P., Schweiger, H.F.: Design aspects and thermomechanical behaviour of converter linings, in german, *Radex-Rundschau*, **45**, 327 – 342, (1990).

27 Schacht, C.A.: Thermomechanical Behaviour of Refractories. *Key Eng. Mat.*, **88**, 193 – 218, (1993).